Differential Geometry for Morphological Analysis of the Built Environment: a Reproducible Workflow to Standardise the Interpretation of Point Clouds

Alessio Cardaci[1,2], Pietro Azzola[1]

[1] University of Bergamo, Engineering and applied Scinces Dept., Bergamo, Italy - (alessio.cardaci, pietro.azzola)@unibg.it
[2] Institute for Construction Technologies, Italian National Research Council, L'Aquila, Italy - cardaci@itc.cnr.it

Keywords: 3D survey, built environment, geomorphometry, deformation analysis, slope and curvature descriptors.

Abstract

Point clouds are now a primary geometric basis for documenting the built environment; however, their analytical value is often constrained when points are treated as mere sets of 3D coordinates, without considering their local behaviour within a neighbourhood. This paper addresses this limitation through a reproducible, robust, and comparable workflow grounded in differential geometry, aimed at deriving slope and curvature descriptors via the numerical estimation of first and second derivatives. The framework supports coherent reading and comparison across datasets: surveys acquired through terrestrial laser scanning and photogrammetry are homogenised and denoised; normal vectors and normal-orientation fields are computed; directional assessments are then performed by extracting profiles along section planes, where controlled smoothing enables stable estimates of derivatives and curvature.
Numerical processing combines open-source tools for point cloud handling with scripted routines (Python for automation and MATLAB for profile-based calculations). The method is validated on three experimental case studies, differing in scale and domain: (i) the Gleno Dam in Val di Scalve, where slope and curvature maps support the identification of local anomalies and discontinuities; (ii) the bridge over the Carso stream in Nembro, compared with an idealised geometry to assess as-built deviations and behaviour in terms of inflection points and curvature inversions; and (iii) a geotechnical laboratory test on a sandy-slope model conducted in a centrifuge, where pre-/post-test comparisons reveal anisotropic deformation trends and associated curvature variations. The contribution also discusses the influence of key parameters and outlines future developments towards fully open-source implementations and AI-assisted morphological interpretation.

1. Introduction

The numerical analysis of point clouds is a core component of digital surveying and three-dimensional representation in architecture and structural engineering. In contemporary 3D models—characterised by high information density, increasingly accurate metric control, and growing internal consistency—spatial information no longer serves solely as a geometric description of reality but becomes an informative resource for morphological reading and interpretation. A point cloud is therefore not merely a discrete set of coordinates: it is a queryable structure that supports investigative operations beyond figurative aims, enabling a broader understanding of the built environment. The *point* acts as an indicator of the discrete sampling of a surface and, through controlled abstraction, is transformed into an algebraic relation that can be examined conceptually and mathematically. The *skin* is not simply reconstructed; it becomes an object of study (and a means for study). First derivatives describe local change within a neighbourhood and are associated with slope and aspect; second derivatives, by contrast, capture intrinsic behaviour through curvature, allowing planar, concave, and convex regions to be distinguished, as well as transitions and discontinuities to be identified.

This approach is rooted in classical differential geometry, beginning with the foundational contribution of Carl Friedrich Gauss. He argues that knowledge of the surface derives not from its global configuration but from the way it changes locally (Gauss, 1828). The implications are immediate: only by numerically reconstructing infinitesimal change does a surface acquire coherent and interpretable geometric meaning. Derivative-based indicators should thus not be seen as merely additional attributes, but as conceptual tools that enable methodologically grounded interrogation of geometry. In continuity with this perspective, Bernhard Riemann reinforces the idea that the geometric characteristics of a space arise from local relations among its components; metric properties are, consequently, founded on infinitesimal relations between contiguous elements (Riemann, 1867). Felix Klein further emphasises that geometry should not be understood as the study of rigid figures, but rather as the study of logical behaviours that remain invariant under transformations (Klein, 1872). Although developed in an abstract context, this paradigm is particularly relevant to digital surveying, where tools derived from differential calculus established geometric principles: slope describes the magnitude and direction of change, whilst curvature reveals intrinsic behaviour and stability. Numerical analysis, therefore, responds not to purely computational demands but to the need to make explicit and measurable those infinitesimal variations which, in the tradition of differential geometry, contain the most informative clues about the structure of the built environment.

2. Differential Geometry and Geomorphological Descriptors

The differential analysis outlined in the preceding theoretical framework becomes fully operational when a surface is not described by an analytical expression, but is reconstructed from a point cloud, that is, from a generally irregular discrete sampling. Differential quantities do not depend on an isolated point, but on the configuration of neighbouring points. They are shaped by local geometry and vary with both the size of

the neighbourhood considered and the level of approximation adopted. Applying differential calculus to point clouds therefore entails a controlled numerical transposition, influenced by the scale of analysis and the extent of the region under investigation. Its outcomes are strongly conditioned by sampling density, noise, the presence of outliers, and the regularisation rules and criteria adopted.

Geomorphometry, the discipline that quantitatively describes landscape forms through morphological indices, provides an important precedent for the study of point clouds (Xiong et al., 2022). Here too, a discrete sampling of a surface can be transformed into derived measures (e.g., slope and curvature) that support an objective interpretation of the constructive features of the surveyed environment. Between the 1970s and 1980s, the field developed a range of operators for form analysis by applying numerical procedures to sampled data (Evans, 2019), (Zevenbergen and Thorne, 1987), (Pike, 1988). Although conceived of natural landscapes, this methodological framework is now readily extendable to the built heritage. Early computational models were largely based on regular grids derived from cartographic representations. Subsequent approaches also considered the area surrounding vertices, using it to estimate the attitude of the tangent plane and the direction of the normal vector. Today, processing commonly relies on approximating the surface by means of a scalar function defined over a 2D (or 2.5D) domain; from this representation, spatial derivatives yield morphometric descriptors capable of characterising form. These descriptors do not merely add numerical values: they make explicit geometric properties that, through morphological inspection alone, would remain difficult to observe or to identify. *Two broad* categories are typically distinguished: *derivative descriptors* (slope, aspect, curvature) and *morphometric indices* (obtained through analytical combinations of other quantities). Their interpretation, however, is tightly scale-dependent, because derivative estimates vary with the extent of the adopted neighbourhood.

First derivatives provide descriptors of slope and aspect, both attributable to the local gradient. Slope measures the magnitude of elevation change; geometrically, it corresponds to the norm of the gradient and therefore expresses the intensity of local change with respect to the tangent plane. Aspect, by contrast, describes the direction of the maximum gradient and indicates the direction of change. In the case of built heritage, these descriptors have important diagnostic value because they enable discontinuities and changes in orientation to be identified—whether intentional (as in edges, mouldings, and joints) or incidental, including those related to ageing (deformations and irregularities arising from settlement and/or deterioration processes). The choice of neighbourhood remains decisive and must be both justified and consistent: a neighbourhood that is too small makes the estimate unstable and sensitive to noise, whereas an overly large neighbourhood tends to filter out detail and produces an excessively smoothed description of form.

Second derivatives yield measures of curvature, which, like slope, depend on the direction chosen on the surface and make it possible to highlight bending, transitions, and changes in morphological regime, distinguishing concave, convex, or near-planar regions. Curvature is therefore not unique and may be adopted as an operational descriptor of local behaviour along a single direction; it should always be interpreted in relation to neighbourhood size and the degree of approximation. Robustness also depends on data quality: noise and outliers can significantly compromise the stability of second-derivative estimates, which are typically more sensitive than first-derivative ones. In architectural and engineering applications, curvature descriptors enable the detection of minute variations in surface geometry and are fundamental for recognising roughness, material loss, localised deformations, and discontinuities between portions exhibiting homogeneous behaviour.

In addition to *derivative descriptors*, geomorphometry also considers *morphometric indices* derived from analytical relationships among basic quantities. The most important indices applied to built heritage include *Topographic Position Index*, which measures a point's relative position with respect to its neighbourhood; *Terrain Ruggedness Index*, which quantifies local roughness through mean elevation variability; and *Relative Slope Position*, which expresses relative placement along a slope. In specific cases, further indices such as *Curvedness* and *Shape Index*, derived from the principal curvatures, are useful: they provide dimensionless measures of local form and distinguish spherical, cylindrical, or planar components (Koenderink and Van Doorn, 1992). These indices facilitate comparison among surfaces and support segmentation into classes.

Recent methods for estimating local normals directly on point clouds, based on decomposing the covariance matrix computed over a neighbourhood, make it possible to convert plane orientation into two scalar quantities: *Dip* and *Dip Direction*. Geometrically, *Dip* represents the inclination angle that the tangent plane forms with the horizontal, measured along the line of maximum slope; *Dip Direction* is the azimuth of the dip direction, i.e., the direction in which the plane descends most rapidly (Mitra and Nguyen, 2003), (Mitra et al., 2004). For built heritage, *Dip* and *Dip Direction* allow continuous measurement and visualisation of deviations and deformations relative to a reference model (out-of-plumb and out-of-level conditions, local inflections, deformations, and misalignments between nominally coplanar portions). This supports both segmentation into surfaces exhibiting homogeneous behaviour and quantitative comparison with a design model.

More recent algorithms, based on the computation of first- and second-order directional derivatives, enable pointwise measurement of how slope, aspect, and curvature vary along specific directions. The surface can thus be analysed anisotropically, accounting for both orientation and the scale of analysis. Moreover, comparing datasets acquired at different times introduces a temporal dimension to morphological analysis, making it possible to identify progressive changes, prevailing directions of deformation, and trajectories of deterioration over time (Hu et al., 2020), (Amatulli et al., 2020). From this perspective, differential geometry applied to digital surfaces emerges not only as a means of computing local attributes, but also as an interpretative method for comparing different phases and for reading transformations of form.

3. Operational Protocol Applied to Point Clouds

Defining a specific and replicable protocol for the "differential" processing of point clouds, aimed at integrating data into numerical-computation software, required the design of a rigorous, disciplined, and meticulous workflow. The point clouds were resampled to ensure homogeneous density, regular

point spacing, and noise reduction (Pesci et al., 2022), by optimising selection parameters, reprojection errors, and reconstruction accuracy. This procedure ensured consistency between data derived from terrestrial laser scanning and photogrammetric capture (Russo et al., 2014). The models were streamlined by removing unnecessary information—such as colour and reflectance—retaining only spatial coordinates. The entire process was carried out using open-source software, in order to obtain a single, acquisition-independent data format that can be readily applied across different contexts.

The methodological core of the process lies in the transformation from the geometric domain to the numerical one: the point cloud, as an expression of the material form and spatial configuration of the built environment, is translated into matrices of values that quantitatively describe surface variation. These operations yield a dataset that does not reproduce the object's physical geometry as such, but rather describes and visualises its behavioural properties. From this perspective, drawing becomes an instrument of analysis and interpretation, capable of making perceptible phenomena that are not evident in geometric restitution alone.

The aim of the workflow is therefore to measure and make comparable—according to criteria of standardisation, traceability, and replicability—changes in orientation, irregularities, and potential deformations. Result quality is assessed against three main criteria. First, repeatability: given the same inputs and parameters, the process must deliver consistent outputs, minimising variability introduced by manual steps or implicit choices. Secondly, robustness: understood as the capacity to maintain interpretative stability even in the presence of noise, non-uniform point density, or differences between acquisitions. Thirdly, comparability: indicators and outputs are constructed to enable direct comparisons between different datasets and between different phases of the same object, ensuring consistent scale, sampling criteria, and output formats. Within the workflow, slope and curvature are computed and used as primary indicators; these descriptors are useful both for morphological analyses (recognising forms and irregularities) and for operational needs such as planarity control, deformation diagnosis, and support for interpreting issues that may be relevant from a conservation or structural standpoint (Yang et al., 2017).

The workflow maintains two complementary levels, consistent with the theoretical framework outlined above: 3D surface analysis and directional, section-based analysis.
The first level consists of a 3D surface reading, aimed at providing a global diagnosis of orientation and local discontinuities. Conceptually, geometry is interrogated by estimating local surface attitude from point neighbourhoods; this enables the production of synthetic orientation maps and the rapid identification of rotations, changes in attitude, and areas where the surface exhibits anomalous or differentiated behaviour. At this stage, point-cloud processing and visualisation tools (e.g., CloudCompare) are used for inspection, quality control, and pre-processing, as well as for computing normals and generating orientation maps—such as Dip and Dip Direction—to support diagnosis and segmentation (Antova and Peev, 2024).
Alongside the three-dimensional reading, the method includes a second analytical line based on sections extracted along principal axes or along particularly representative directions. This choice is motivated by an operational requirement: in many technical contexts, planar sections remain the most effective instrument for dimensional verification and for communicating results. Section-based analysis enables a more controlled and legible profile reading, reducing interpretative ambiguities that are typical of three-dimensional maps alone. Moreover, by constraining analysis to a defined trace, the influence of adjacent portions of the point cloud that might introduce irrelevant disturbances (lateral elements, noise, out-of-plane components) is limited. In this sense, section-based reading does not replace the three-dimensional one, but complements it: the former makes comparison along a chosen direction more rigorous, whilst the latter maintains a global view of the surface.

Operationally, section analysis is performed via a MATLAB script that selects points within a narrow band, orders them along the profile direction, and reconstructs a continuous trend through a smoothed curve, so as to derive indicators consistent with slope and curvature. The slope of a curve $z = f(x)$ is defined as the first derivative:

$$\mathrm{w} = \frac{dz}{dx}. \tag{1}$$

In three-dimensional contexts, slope corresponds to the magnitude of the gradient of a surface:

$$\kappa = \frac{d^2 z}{dx dy}. \tag{2}$$

The physical interpretation of these parameters is more immediate:

1. Slope expresses the change in elevation relative to horizontal distance. It quantifies local inclination and, in physical terms, represents the energy required to overcome a rise, the stability of a slope, or the resistance to flow. In architectural or territorial surveys, slope serves as a key indicator of the morphology of both built and natural environments (1).
2. Curvature, calculated through the second derivative, describes the rate at which a line or profile changes direction in space. It is directly related to concepts of stability and stress: high curvature values correspond to ridges, depressions, or edges, which often mark zones of instability or stress concentration. In architecture and structural engineering, curvature highlights areas of deformation and discontinuity, offering insights into the static and dynamic behavior of built systems (2).

The differential analysis of XYZ data through slope and curvature provides an effective framework for interpreting surface geometry and behavior. Slope describes local inclinations, whereas curvature captures directional variations, enabling the identification of significant morphological features. When combined, these parameters allow a transition from basic geometric measurements to higher-level knowledge, supporting applications that range from built heritage documentation to geotechnical modeling, structural analysis, and territorial management. In common open-source and licensed software environments, slope and curvature are computed directly on point clouds by first estimating a unit normal vector at each point within a user-defined neighborhood (e.g., k-nearest neighbors or fixed-radius search). Using a standard least-squares plane fitting approach, the local covariance matrix is defined as

$$\mathbf{C} = \frac{1}{n} \sum_{i=1}^{n} (\mathbf{p}_i - \bar{\mathbf{p}})(\mathbf{p}_i - \bar{\mathbf{p}})^{\mathrm{T}}, \tag{3}$$

where $\mathbf{p}_i$ are the neighboring points and $\bar{\mathbf{p}}$ is their centroid. The unit normal vector $\hat{\mathbf{n}}$ is obtained as the eigenvector corresponding to the smallest eigenvalue of $\mathbf{C}$. Normal orientation can be consistently propagated using a preferred axis, sensor viewpoint constraints, or minimum spanning tree strategies.

Local slope is derived from the gradient of the fitted plane, while curvature can be estimated either through local quadric surface fitting or by eigenvalue-based descriptors, with principal curvature directions given by the associated eigenvectors. The combined use of slope and curvature therefore represents a robust and interdisciplinary methodological tool, supporting both scientific investigation and operational workflows in engineering, architecture, and conservation.

The implementation strategy is based on a Python-driven workflow that programmatically generates MATLAB scripts to produce advanced plots and derived representations of surveyed point-cloud models. Python is used for data mediation, automation, and workflow control, while MATLAB provides robust numerical processing and publication-quality visualization capabilities. Beyond omnidirectional neighborhood analysis, the methodology introduces a directional estimation of slope and curvature constrained to user-defined planar sections. This approach enables the analysis of thin, targeted slices of the point cloud, reducing the influence of adjacent or disturbing elements and yielding section-specific geometric descriptors. By restricting computations to selected profiles, the method complements surface-based metrics with section-aligned slope and curvature information.

The workflow is applied to a geotechnical case study comparing pre- and post-test point clouds. Longitudinal sections exported as ASCII tables are processed by fitting smoothed cubic splines, from which first and second derivatives are computed, visualized, and exported, supporting standardized analysis and operator-oriented reporting.

3.1 Inputs and key parameters

The workflow operates on planar sections exported from CloudCompare as ASCII files containing three-dimensional coordinates. Two datasets are considered, corresponding to the initial and final survey epochs. The target section is defined by a nominal midline along the Y axis and by a narrow selection band that isolates a thin slice of the point cloud $y_0 = v$.

The half-thickness of the section is controlled by a tolerance parameter δ, and points are retained only if their coordinates satisfy the following condition:

$$y_0 - \delta < Y < y_0 + \delta \tag{4}$$

The selected points are processed along the section direction by fitting a cubic smoothing spline, whose behavior is governed by a smoothing parameter p:

$$0 < p < 1. \tag{5}$$

3.2 CSAPS Smoothing spline formulation

A key issue concerns smoothing, introduced to ensure robustness: when local-variation indicators are derived, noise may be amplified and translate into interpretative instability; smoothing is therefore adopted as a controlled and coherent regularisation procedure (Broberg et al., 2025).

The cubic smoothing spline $s(x)$ is computed by minimizing a functional that balances fidelity to the measured data and global smoothness:

$$p \sum_{i=1}^{n} w_i \big(y_i - s(x_i)\big)^2 + (1-p) \int \big(s''(x)\big)^2 \, dx. \tag{6}$$

The first term enforces adherence to the observed data, while the second penalizes excessive curvature. Values of p close to unity result in an almost interpolatory spline, suitable for high-quality survey data, whereas lower values increase smoothing at the expense of pointwise accuracy (figure 1). With $p \to 1$,

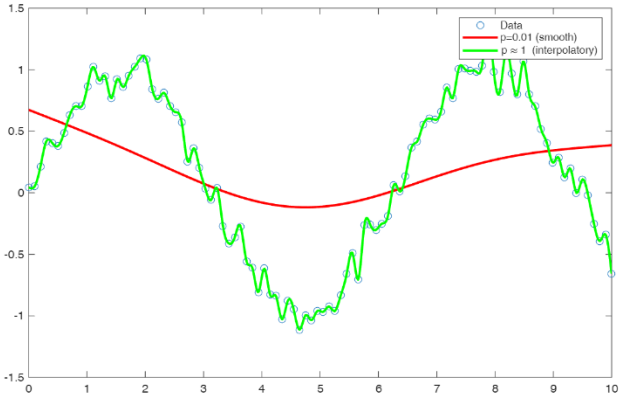

Figure 1. Effect of the smoothing parameter p in MATLAB's `CSAPA`.

the spline closely follows the measured profile, enabling reliable estimation of first- and second-order derivatives (slope and curvature proxies) along the selected section (Figure 1).

3.3 Core routine: process section

All processing steps for a single dataset are encapsulated in a dedicated routine that returns uniformly sampled profiles, first and second derivatives, cleaned input points, and the spline model:

$$\big(x_q, z_q, dz, ddz, x_\mathrm{u}, z_\mathrm{u}, sp\big) = \mathrm{p\_s}(\mathrm{filename}, y_0, \delta, p). \tag{7}$$

After importing the point cloud section as a set of coordinates (X, Y, Z), a thin planar strip is isolated around the target section midline by enforcing the selection criterion:

$$y_0 - \delta < Y < y_0 + \delta. \tag{8}$$

The retained points are sorted along the abscissa and deduplicated to ensure a single-valued mapping $Z = f(X)$, which is required for one-dimensional spline fitting. A cubic smoothing spline $s(X)$ is then fitted to the cleaned data:

$$Z = s(X), \qquad s \in \mathcal{C}^2, \tag{9}$$

with smoothing controlled by the parameter p. The spline is evaluated on a uniform query grid defined over the observed domain:

$$x_q \in [\min(x_\mathrm{unique}),\, \max(x_\mathrm{unique})]\,. \tag{10}$$

From the fitted spline, the profile and its derivatives are computed as:

$$z_q = s(x_q), \qquad dz = \frac{dZ}{dX}, \qquad ddz = \frac{d^2Z}{dX^2}. \tag{11}$$

The routine is applied independently to the initial and final survey epochs, yielding two comparable sets of profiles, slopes, and curvature proxies.

A reference design polyline $\{x_{\mathrm{ref}}, z_{\mathrm{ref}}\}$ is used for comparison, and piecewise slopes are computed by finite differences:

$$m_k = \frac{z_{\mathrm{ref},k+1} - z_{\mathrm{ref},k}}{x_{\mathrm{ref},k+1} - x_{\mathrm{ref},k}}, \qquad k = 1, \ldots, n-1. \tag{12}$$

The resulting profiles and derivatives are visualized in three diagnostic panels (profile, slope, curvature) and exported both as polyline files and as structured tables in an Excel workbook, providing a standardized and operator-oriented output for further analysis.

The workflow also includes comparison with a reference profile (design or expected), which is useful for assessing deviations in a direct and communicable manner. Outputs are organised in graphical and tabular forms, with exports in simple formats (tables and plots) to facilitate interoperability and reuse in reports or subsequent analyses. The method integrates a level of automation in Python, with the aim of standardising repetitive steps (file selection, path definition, parameters, and output naming) and reducing human error, thereby ensuring consistency across successive runs. In addition, a wizard with a graphical user interface guides the user in selecting inputs and defining essential parameters, automatically generating a pre-filled MATLAB script. In this way, the procedural dimension is not left to contingent choices, but channelled into a workflow that can be verified at every step. The methodology is not configured as a sequence of isolated operations, but as an integrated framework that renders geometry measurable, readable, comparable, and communicable, maintaining a balance between rigour and practicality.

Three-dimensional analysis provides a global diagnosis of surface attitude and discontinuities, whilst section-based analysis enables targeted checks and detailed comparisons. The method nonetheless has intrinsic limitations: section-based indicators depend on the quality of the reconstructed profile and on smoothing choices; moreover, curvature should be understood as an operational indicator of profile variation—useful for highlighting critical areas—but one that must be interpreted with caution when drawing broader conclusions about the surface as a whole. Explicitly stating these constraints, together with standardising operational choices and enabling the workflow to be repeated under controlled conditions, constitutes an essential part of the methodological value of the proposed framework.

3.4 Python-assisted generation of MATLAB scripts for dimensional analysis

A dedicated Python-based utility was developed to automate the generation of MATLAB scripts used for dimensional verification and numerical analysis (Figure 2). The tool implements a GUI-driven wizard that guides the user through data selection, parameter definition, and output configuration, producing a ready-to-run `.m` file.

The workflow includes: (i) selection of pre- and post-intervention datasets; (ii) validated acquisition of geometric and numerical parameters defining the section extraction and smoothing strategy; (iii) optional definition of a reference polyline; and (iv) standardized configuration of output files and paths. All inputs are checked for consistency and formatted to ensure direct compatibility with MATLAB syntax.

This approach minimizes manual editing, reduces the risk of transcription errors, and ensures reproducibility of the analysis pipeline. The generated MATLAB script constitutes the entry point for the analytical procedures described in Section **??**, where dimensional deviations are computed against reference or design models.

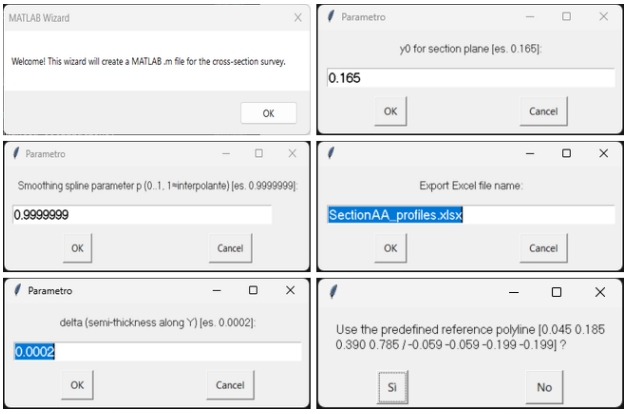

Figure 2. GUI of the Python wizard for automated generation of MATLAB scripts dimensional analysis workflow.

3.5 Analytical workflow for structural thickness analysis from raster profiles

The workflow provides an automated framework for the metric analysis of arch dam cross-sections from raster data, with operator input limited to ROI definition. Raster sections are scaled through a fixed pixel-to-metric factor s (m/px), and edge pixels are extracted via Canny detection.

Within each ROI, upstream and downstream intradoses are modelled as ideal circular arcs using a robust two-stage fitting strategy (bounded RANSAC followed by algebraic refinement), yielding the parameters $(\mathbf{C}_D, R_D)$ and $(\mathbf{C}_U, R_U)$. Radial thickness is computed analytically by casting rays from the downstream centre,

$$\mathbf{X}(t) = \mathbf{C}_D + t\,\mathbf{u}(\varphi) \tag{13}$$

and solving the ray-circle intersection with the upstream intrados. The thickness is defined as

$$t(\varphi) = t^\star(\varphi) - R_D \tag{14}$$

where $t^\star(\varphi)$ is the smallest positive intersection, accounting for non-concentric geometries.The adherence of real pixels to the ideal model is quantified through the radial residual

$$\Delta r = \|P - \mathbf{C}\| - R \tag{15}$$

analysed as a function of the angular coordinate φ within a structurally relevant sector. Global comparisons across arches

include the evaluation of centre displacement vectors

$$\Delta \mathbf{C}_i = \mathbf{C}_{U,i} - \mathbf{C}_{D,i} \tag{16}$$

The results confirm the suitability of circular modelling while revealing measurable thickness variations and centre offsets.

4. Study Cases

Tre Three representative experiences—the Gleno Dam, the bridge over the Carso stream in Nembro, and a laboratory geotechnical test on a sandy-slope model—illustrate the application and progressive integration of modelling, computation, and representation.

4.1 The Gleno Dam

The investigation focused on the morpho-logical analysis of the main body and the internal cylindrical surfaces, with particular attention to the inclination (slope) of the segments and to the curvature of horizontal sections. Point clouds acquired through TLS and UAV systems were processed to compute first- and second-order derivatives, producing slope and curvature fields that supported the recognition of planimetric deformations and local anomalies.

In particular, the combined reading of the two indicators made it possible to distinguish gradual geometric variations from sharper changes attributable to surface discontinuities or constructive irregularities (Figures 3 and 4). Overall, the assessment yielded a coherent three-dimensional model suitable for subsequent numerical simulation and structural monitoring, in which discontinuities and anomalies emerged that would otherwise have been difficult to identify (Figure 5). This outcome confirms the value of moving from a topographic description to a differential reading, in which *form* is interpreted as a measurable signal that can be compared over time.

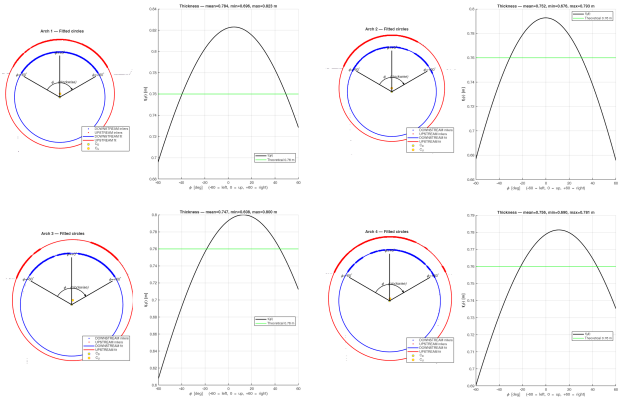

Figure 3. ROI-based interpolation of upstream and downstream circular intradoses and corresponding radial thickness distribution.

4.2 The bridge over the Carso stream in Nembro

The survey aimed to compare the actual geometry with the theoretical design geometry, in order to assess as-built fidelity and detect potential deformations (Figure 6).

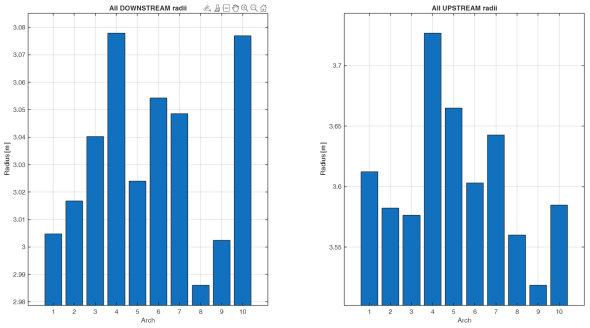

Figure 4. Downstream vs. upstream radii of curvature of the dam arches.

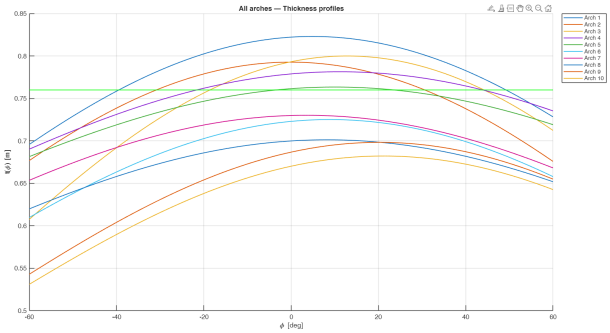

Figure 5. Comparison of the arch profile evolution with respect to the design thickness.

Differential analysis made it possible to determine local deviations of the intrados, whilst examination of slope and curvature revealed changes in inclination and geometric discontinuities (Figure 7). It emerged that the arch was not constructed using regular curved formwork, but rather through straight formwork elements approximating a piece-wise-linear profile.

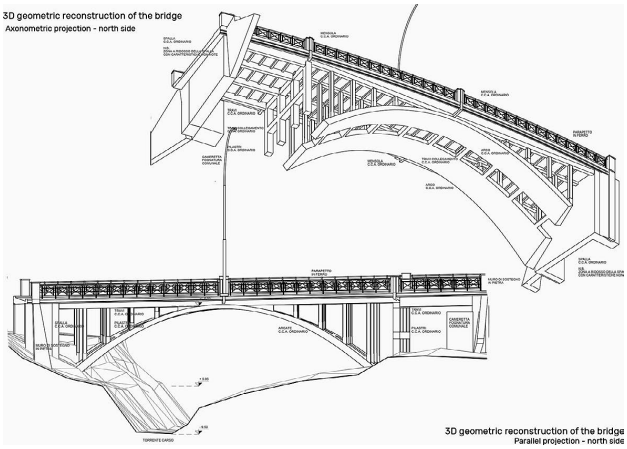

Figure 6. Axonometric structural representation of the bridge.

This construction solution generated inflection points and potential stress concentrations. Beyond documenting the discrepancy between the theoretical model and the actual configuration, the results show how differential indicators can relate a *geometric deviation* to a plausible construction cause, providing quantitative support for subsequent structural checks.

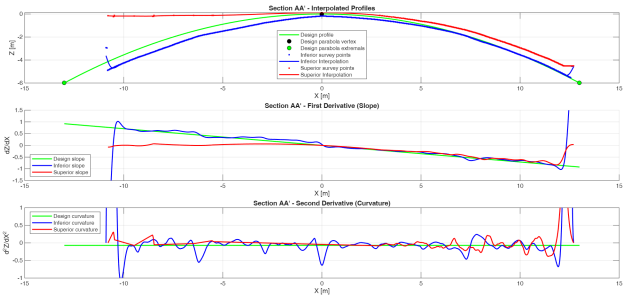

Figure 7. Interpolation of the longitudinal bridge profile and computation of $z(x)$, $z'(x)$, and $z''(x)$ for curvature assessment.

4.3 Laboratory geotechnical test on a sandy-slope model

This case study concerns a scaled model of a sandy slope subjected to dynamic loading in a geotechnical centrifuge (Figure 8). Comparing three-dimensional models acquired pre- and post-event made it possible to measure displacements and differential deformations (Figure 9).

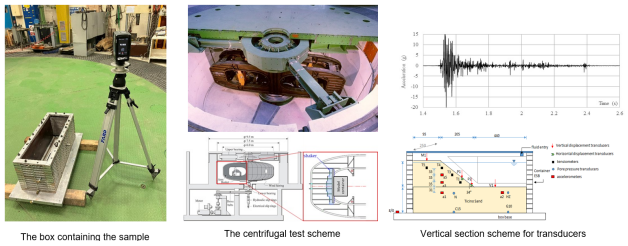

Figure 8. Geotechnical test specimen and schematic layout of the testing procedure.

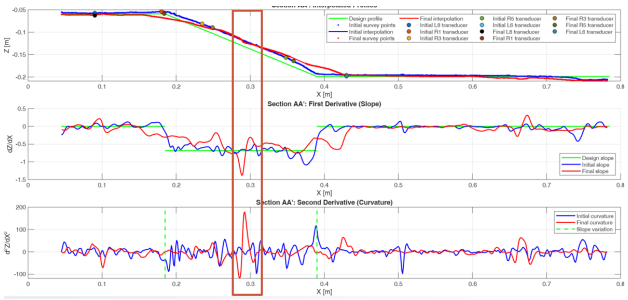

Figure 9. Interpolation of the longitudinal axis profile and computation of $z(x)$, $z'(x)$, and $z''(x)$ for curvature assessment.

Directional derivatives enabled an anisotropic reading of the deformation phenomena, identifying prevailing movement directions and areas of stress concentration (Figure 10). The case study provides an application of the algorithm previously presented, applied to a specimen at a much smaller scale, with overall dimensions below one metre, and requiring a significantly higher survey resolution. The aim is to highlight both the macroscopic mechanisms of the slope and the microscopic behaviour of the soil grains.

The experimental campaign is designed to enhance the readability of deformations before and after the seismic event of the test, with reference to a predefined design geometry. The test made it possible to identify the actual soil displacements by comparing them with instrumental readings obtained from displacement transducers installed within the specimen, and to define a specific survey protocol for extracting longitudinal and transverse sections at known distances.

This behaviour is clearly identifiable through numerical analysis, which can capture even minimal mechanical effects that are not visually detectable.

In this sense, curvature does not merely describe how much the surface bends; it becomes an indicator of the distribution and localisation of change, useful for interpreting the system's response under loading.

Across different domains—historic structures, reinforced-concrete infrastructure, and experimental geotechnical modelling—the three cases confirm that differential surface representation enables a shift from purely metric restitution to morphological diagnosis: slope highlights gradients and transitions; curvature captures inflections, discontinuities, and local anomalies; and comparison between design and as-built conditions renders discrepancies and differences measurable.

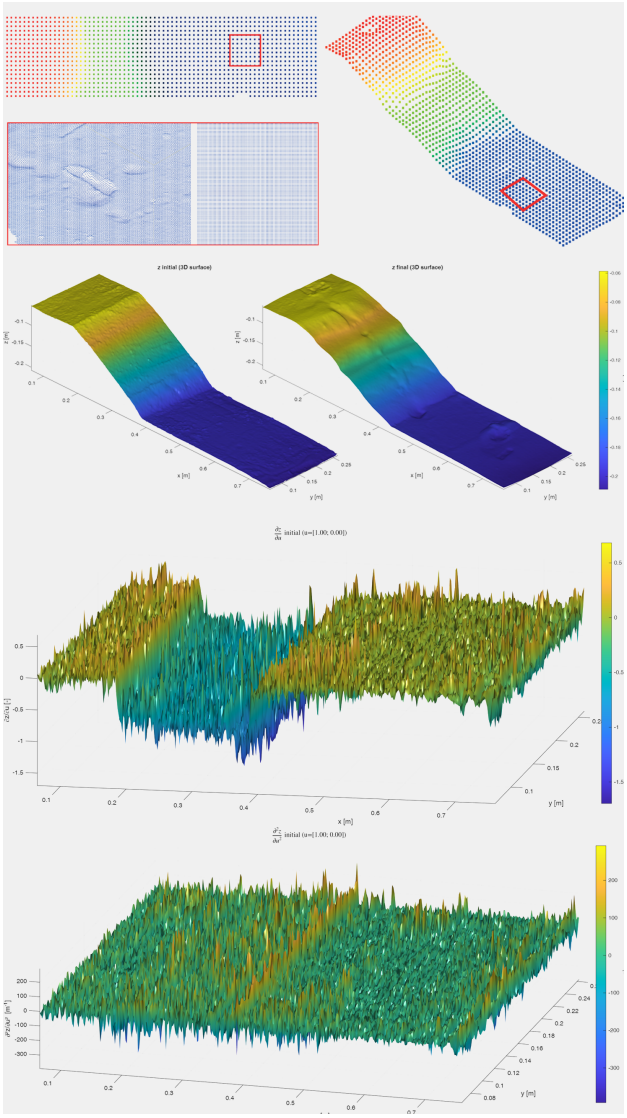

Figure 10. Point cloud sampling Definition of the function and its bidirectional and unidirectional derivatives along the longitudinal axis.

5. Conclusion

The proposed approach is characterized by a high degree of methodological rigor and by the advantages it offers over traditional techniques for morphological analysis. Modeling the surface mathematically as a continuous function makes it possible to interpret geometry in quantitative terms, moving beyond a purely topographic description. Integrating heterogeneous tools (Python, MATLAB, and CloudCompare) enables the construction of a scientifically reproducible procedure, although it requires advanced technical expertise and careful management of software dependencies.

Sensitivity to noise and sampling density constitutes an intrinsic limitation, which can be mitigated through dynamic calibration of smoothing parameters and by optimizing the extent of the neighborhood area. This, in turn, highlights the need for a preliminary data-quality control phase, in which parameter selection is not a "graphical" act, but a traceable and justified methodological decision. Differential analysis of point clouds defines a shared numerical language for three-dimensional representation, in which slope and curvature assumes the role of universal measures of form. Grounded in the link between first- and second-order derivatives, this language opens new possibilities for dialogue across related disciplines (drawing, geomatics, geotechnics, and the physics of materials), fostering a more unified approach to morphological interpretation.The workflow outlined here integrates differential calculus, scientific programming, and interactive visualization, proposing a model that is applicable both to research and to operational practice in architectural and environmental surveying.

Within this framework, the presented case studies provide an empirical verification of the method's transferability: objects and scales vary, yet the ability to translate form into comparable and interpretable indicators remains constant.

Future perspectives concern the development of fully open-source pipelines and the use of artificial intelligence algorithms for automated morphological analysis. In this direction, the correlation between geometric function, derivatives, and physical behavior is confirmed as a key element of scientific surveying capable of integrating the objectivity of measurement with the interpretative depth of analysis. The goal is to consolidate an operational ecosystem in which acquisition, computation, and visualization converge into a transparent, replicable, and scalable chain, useful for both diagnostics and monitoring.

6. Transparency Statement

The authors declare that artificial intelligence tools ChatGPT (OpenAI) and DeepL Write (DeepL) were used solely for minor language editing (grammar, spelling, and readability), and that all changes were reviewed and approved by the authors. No scientific content, analyses, results, or interpretations were generated by AI. The authors take full responsibility for the integrity and accuracy of the manuscript.

References

Amatulli, G., McInerney, D., Sethi, T., Strobl, P., Domisch, S., 2020. Geomorpho90m, empirical evaluation and accuracy assessment of global high-resolution geomorphometric layers. *Scientific Data*, 7(1), 162.

Antova, G., Peev, I., 2024. Comparison on Commercial and Free Software for Point Cloud Processing. *Inżynieria Mineralna*, 1(1), 511–519.

Broberg, P. H., Lindgaard, E., Olesen, A. M., Jensen, S. M., Stagsted, N. K., Bjerg, R. L., Grosselle, R., Oca, I. U., Bak, B. L., 2025. HISAPS: High-order smoothing spline with automatic parameter selection and shape constraints. *SoftwareX*, 29, 102049.

Evans, I. S., 2019. General geomorphometry, derivatives of altitude, and descriptive statistics. *Spatial analysis in geomorphology*, Routledge, 17–90.

Gauss, C. F., 1828. *Disquisitiones generales circa superficies curvas*. 1, Dieterich.

Hu, G., Dai, W., Xiong, L., Tang, G., 2020. Classification of terrain concave and convex landform units by using TIN. *GEOMORPHOMETRY 2020*, 46.

Klein, F., 1872. Vergleichende Betrachtungen über neuere geometrische Forschungen. *Vergleichende Betrachtungen über neuere geometrische Forschungen*.

Koenderink, J. J., Van Doorn, A. J., 1992. Surface shape and curvature scales. *Image and vision computing*, 10(8), 557–564.

Mitra, N. J., Nguyen, A., 2003. Estimating surface normals in noisy point cloud data. *Proceedings of the nineteenth annual symposium on Computational geometry*, 322–328.

Mitra, N. J., Nguyen, A., Guibas", L., 2004. Estimating surface normals in noisy point cloud data". *special issue of International Journal of Computational Geometry and Applications*, 14number 4–5, 261–276.

Pesci, A., Teza, G., Loddo, F., Fabris, M., Monego, M., Amoroso, S. et al., 2022. Studio di possibili effetti sistematici nelle nuvole di punti SfM da APR: confronti con TLS, distorsioni e metodi di mitigazione. *QUADERNI DI GEOFISICA*, 177(177), 1–22.

Pike, R. J., 1988. The geometric signature: quantifying landslide-terrain types from digital elevation models. *Mathematical geology*, 20(5), 491–511.

Riemann, B., 1867. Über die Hypothesen, welche der Geometrie zu Grunde liegen. *Abhandlungen der Königlichen Gesellschaft der Wissenschaften zu Göttingen*, 13, 133–152.

Russo, M., Manferdini, A. M. et al., 2014. Integration of image and range-based techniques for surveying complex architectures. *ISPRS Annals of the Photogrammetry, Remote Sensing and Spatial Information Sciences*, 305–312.

Xiong, L., Li, S., Tang, G., Strobl, J., 2022. Geomorphometry and terrain analysis: data, methods, platforms and applications. *Earth-Science Reviews*, 233, 104191.

Yang, H., Omidalizarandi, M., Xu, X., Neumann, I., 2017. Terrestrial laser scanning technology for deformation monitoring and surface modeling of arch structures. *Composite Structures*, 169, 173–179.

Zevenbergen, L. W., Thorne, C. R., 1987. Quantitative analysis of land surface topography. *Earth surface processes and landforms*, 12(1), 47–56.